

We are IntechOpen, the world's leading publisher of Open Access books Built by scientists, for scientists

6,900

Open access books available

186,000

International authors and editors

200M

Downloads

Our authors are among the

154

Countries delivered to

TOP 1%

most cited scientists

12.2%

Contributors from top 500 universities



WEB OF SCIENCE™

Selection of our books indexed in the Book Citation Index
in Web of Science™ Core Collection (BKCI)

Interested in publishing with us?
Contact book.department@intechopen.com

Numbers displayed above are based on latest data collected.
For more information visit www.intechopen.com



The Development of the Multi - Fuel Burner

Anna Maiorova, Aleksandr Sviridenkov, Valentin Tretyakov,
Aleksandr Vasil'ev and Victor Yagodkin
*Central Institute of Aviation Motors named after P.I. Baranov
Russia*

1. Introduction

For modern propulsion engineering the trend to use of a wide spectrum of liquid fuels – both oil, and alternative is characteristic. The physical properties of various liquids corresponding to the Russian and international standards, are resulted in table 1. As we see from table. 1, a range of change of fuel properties, especially viscosity, is wide enough. One of the most pressing problems at present is creation of combustion chambers for engines and gas-turbine plants which can operate on fuel with as low as the increased viscosity at preservation of low level of toxic species emissions.

Liquid	Density, kg/m ³	Kinematic viscosity •10 ⁶ , m ² /s	Surface tension coefficient •10 ³ , N/m
Distilled water	998.2	1.003	72.75
Ethanol	788	1.550	22.3
Kerosene TS1	≥780	≥ 1.3	24.3
Rapeseed oil	916	88.62	33.2
Summer diesel	≤ 860	3.0-6.0	28.9
Winter diesel	≤ 840	1.8-5.0	27.8
FAME (biodiesel)	877-879	8.0	31.4

Table 1. Physical properties of liquids.

Maintenance of the majority of requirements shown to the combustion chamber directly depends on the chosen scheme of spraying system. Fuel ignition at an engine or gas-turbine plant start-up, stability and efficiency of combustion, levels of toxic species emissions are connected with fuel atomization and its mixing with air in atomization system. Several injectors of various types and a whole number of air swirlers various on a design can form modern atomization system. The review of various types of sprayer units and the analysis of the conclusions made in works (Lefebvre, 1985;Vasil'ev, 2007) shows, that the most perspective direction of researches is the development of the device with the pneumatic scheme of an atomization. The main lack of such scheme of an atomization is insufficient droplet's fineness on wake-up modes for assured lighting in combustor. To reach comprehensible droplet's fineness on low modes it is possible to use pressure-swirl injectors

with comprehensible maximum injection pressure (nearby 2 MPa). However at such injection pressure it is impossible to provide all range of operation modes with injectors of this scheme.

The most promising direction of researches is the development of the dual-orifice (on fuel) burner of the combined centrifugal-airblast scheme. The aims of this work are scheme selection, designing, test and research as injectors, and the burner as a whole for low-emission combustors on fuels as usual, as increased viscosity (kerosene, ethanol, diesel, biodiesel)

2. The selection of the sprayer unit scheme

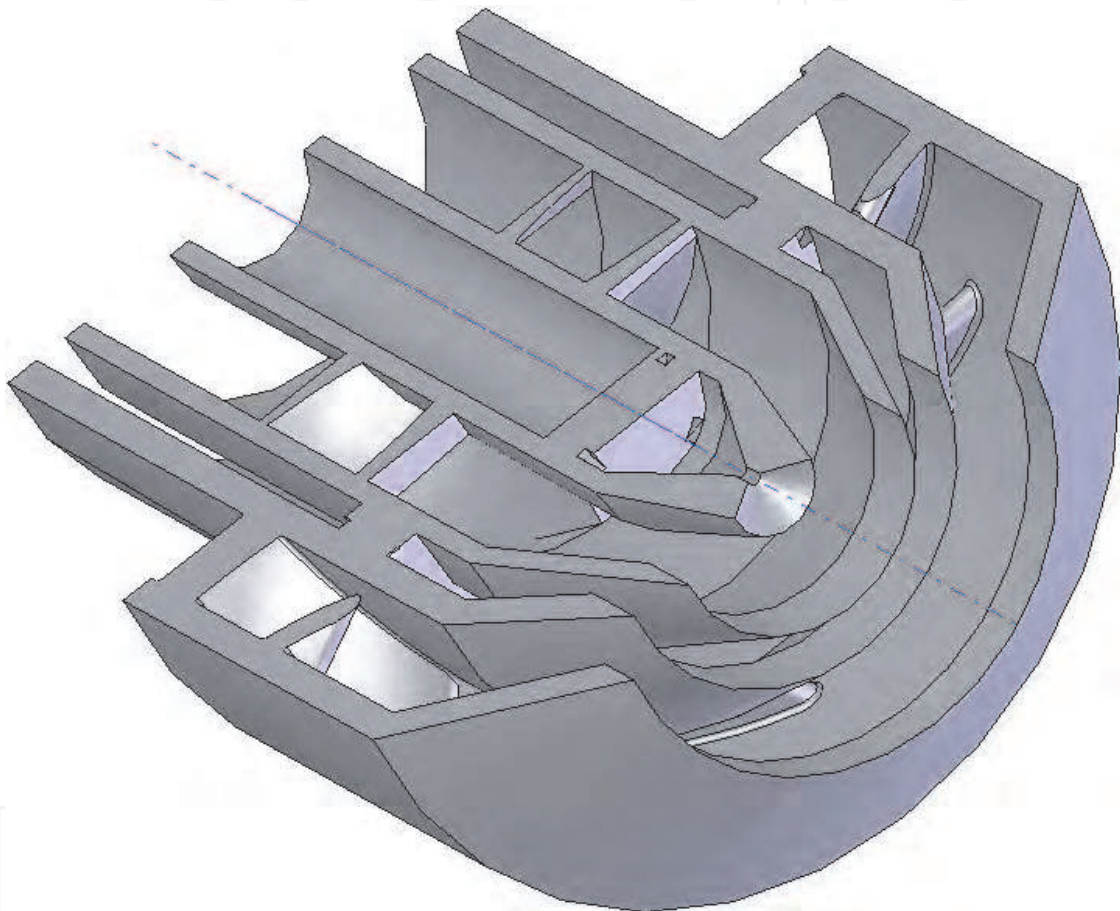


Fig. 1. A scheme of the sprayer unit

The shape of the designed sprayer unit is resulted on fig. 1. Nozzles of injectors place concentrically. The low-rate pilot channel (pressure swirl nozzle) is installed on a burner axis. Confidently to ignite the chamber, it is necessary to provide hit of a quantity of fuel droplets into plug discharge zone. Hence the atomizer should have a large fuel spray angle $2\theta_R$ (80-100°). The main channel – airblast nozzle, is located between two air swirlers for the best crushing of a liquid film and fuel spray stabilization.

Sprayer unit basic elements are shown on fig. 2. The sprayer unit consists of a casing 1, outer air swirler 2 and injector shaft 3. The casing forms an outer air nozzle 4 and the cowling with basic spraying edge 5. Blades of an outer air swirler 2 are disposed on a shaft of a fuel atomizer 3 which in turn contains the channel 6 of main fuel injection with

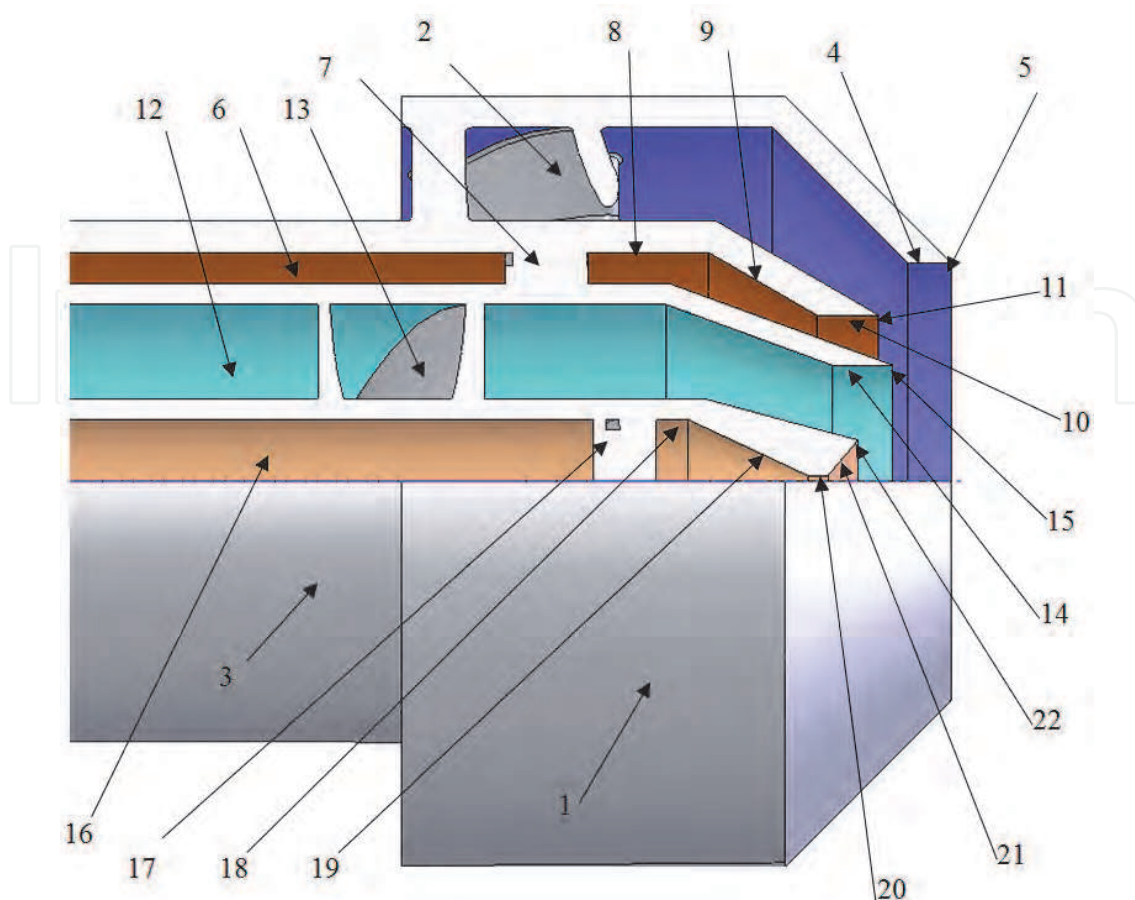


Fig. 2. Basic elements of sprayer unit

disposed in it consistently: fuel auger 7, swirl chamber 8, conic section 9, fuel nozzle 10 of main channel and cowling with spraying edge 11. Concentrically in the channel 6 of main fuel injection there is the channel 12 for air input into the central air passage with the central air swirler 13, the air nozzle 14 and an edge 15 disposed in it. On an injector axis installation of the pilot fuel channel 16 with auger 17, the swirl chamber 18, conical section 19, the nozzle 20, an expansion face 21 and an the cowling with edge 22 disposed in it is possible.

The sprayer unit works by a following principle. The pilot injector works on all power conditions, including provides start. It is offered to execute chamber start at fuel injection pressure of an order 0.5 MPa. On an intermediate mode injection pressure on the pilot channel can even be a little reduced for submission greater fuel shares through the main channel for the purpose of maintenance of the best uniformity of concentration in fuel-air spray. On a wake-up mode fuel moves only in the pilot channel 16 (working as pressure swirl atomizer). There the fuel passing through auger 17 is swirled, merging on length of the swirl chamber of 18 from discrete sprays in a fuel flow. In a conic section 19 fuel flow increases a tangential velocity and reaching a maximum at passage of the nozzle 20 reveals in a conic film. The face 21 helps to increase spray angle on a wake-up mode. . Breaking from edge 22 fuel film disintegrates on drops under the influence of internal (hydrodynamic) forces or to be atomized by external streams of air, depending on the relation of fuel and air momentums. On higher modes the fuel moving in the main channel 6 (operating as airblast atomizer) is swirled in the fuel auger 7, breaks from a spraying edge 11, and the fuel film to be atomized between two swirl streams of air formed by swirlers 2 and 13.

3. The design of the burner

At designing dual-orifice injector device it is necessary to know flow hydraulic characteristics on each of channels. Hydraulic characteristics of an injector are, first of all, the flow rate characteristic: $G_f = G_f(\Delta P_f)$, where G_f - mass flow rate of a liquid, ΔP_f - injection pressure, and the factors connected with it.

Definition of a discharge coefficient of injector C_d is given by the formula

$$C_d = G_f / (f_c \sqrt{2 \rho_f \Delta P_f}), \tag{1}$$

where f_c - the nozzle area on a shear (in narrow section), ρ_f - liquid density
For the pressure swirl channel also it is necessary to calculate assumed drop sizes and a fuel-air spray angle, especially for a wake-up mode where spraying air doesn't yet exert essential influence on a spray.

The root angle θ_R is determined from a condition:

$$\text{tg}(\theta_R) = u_\varphi / u_x, \tag{2}$$

where u_x and u_φ - axial and tangential velocities of a liquid in the centre of a liquid film on an exit from the nozzle. The effective angle θ_e corresponds to an actual corner of projection of drops or a fluid spray cone angle.

After the spray angle and the film width w_e estimation Sauter Mean Diameter of droplets SMD was determined in calculations by Lefebvre formula (Lefebvre A.H., 1989)

$$\text{SMD} = 4.52 \left(\frac{\sigma_f \mu_f^2}{\rho_f \Delta P_f^2} \right)^{0.25} (w_e \cos \frac{\alpha_e}{2})^{0.25} + 0.39 \left(\frac{\sigma_f \rho_f}{\rho_A \Delta P_f} \right)^{0.25} (w_e \cos \frac{\alpha_e}{2})^{0.75} \tag{3}$$

Here μ_f , σ_f - liquid dynamic viscosity and surface tension coefficient, ρ_A - air density.
For selection of fuel rates relation on engine operation modes and the main geometrical characteristics of fuel channels designing hydraulic calculations of pilot and main channels (tab. 2, 3) are carried out. The program *fnozzle*, based on a technique (Dityakin at al., 1977) with some refinements of authors was used. In designing calculation the ideal diesel was considered as fuel ($\rho_f = 845 \text{ kg/m}^3$, $\nu_f = 4.17 \text{ mm}^2/\text{s}$, $\sigma_f = 28.1 \text{ mN/m}$ at $T = 293 \text{ K}$). The injector device was designed on a landing place of 48 mm. On the basis of hydraulic designs the main geometrical characteristics of fuel channels have been chosen. For example, fuel nozzle diameter of a airblast injector has made 22 mm.

No	ΔP_f , MPa	G_f , kg/s	$2\theta_R$ °	SMD, mkm
1	0.0131	0.0008	76.2	177.8
2	0.1068	0.0025	86.0	72.0
3	0.1578	0.0030	87.6	61.2
4	0.3054	0.0041	89.6	47.1
5	0.4713	0.0050	90.9	39.7

Table 2. Hydraulic design of pilot fuel channel

From table 2 it is visible, that on a prospective wake-up mode (injection pressure an order 0.5 MPa) calculated drop size reaches 40 microns and a root fuel-air spray angle of an order 90° (a line 5). On a 100 % mode (a line 4) injection pressure is nearby 0,3 MPa, drop size makes 47 microns, and a root angle - 90°. The reached values should be enough for assured firing of the combustion chamber, taking into account that pressure and temperature in the combustor were considered as the normal.

Nº	ΔP_f , МПа	G_f кг/с	$2\theta_R$, °	SMD, мкм
1	0.0116	0.00250	135.9	300.0
2	0.1039	0.01350	144.9	103.3
3	0.1488	0.01700	146.7	85.0
4	0.3531	0.02500	148.6	58.6

Table 3. Hydraulic design of main fuel channel

Calculation of the main channel is resulted, basically, for the purpose of obtaining of the flow rate characteristic on fuel. As this channel works by a principle of a pneumatic atomization the real sizes of drops will essentially less. Fuel-air spray angle practically will depend completely on a direction of motion of air streams.

Analyzing the calculations carried out , it is possible to choose the fuel rate relation on injector channels for the main operating modes of the combustor (wake-up, underload, mode 100 %). Let's consider, that the maximum mass flow rate on one injector makes 29.1 g/s of diesel fuel. On a wake-up mode the pilot channel with the injection pressure corresponding to a line 5 in table 2 works only. It provides a fuel rate through the injector 5 g/s. On an underload mode, fuel is supplied in the main and pilot channels with identical pressure difference of an order 0,15 MPa (a line 3 in tables 2 and 3). Passing through the pilot channel 3 g/s, through the main - 17 g/s, we will receive the fuel mass flow rate through the sprayer unit 20g/s. On a 100 % mode fuel injection pressure in channels increases to 0.3 MPa (a line 4 in tables 2 and 3). Passing through the pilot channel - 4.1 r/c, through the main - 25 r/c, we will receive the fuel mass flow rate through the device accordingly 29.1 r/c. Thus, the fuel supply in both channels can be carried out by one pump with use of one simple valve. The size of diesel fuel droplets thus, taking into account gas recompression in the combustor, should not exceed 25-40 microns. Such values should provide high combustion efficiency of the diesel fuel moving through pilot and main channels of the burner , on all operational modes of low-emission combustor.

To obtain characteristics of airflows, reverse zone size and to select swirl scheme to the beginning of detail design 3D calculations of device, established in circular pipe, have been conducted by a technique (Patankar, 1980). Air pressure upon an exit from calculation area makes 0,1 МПа. Calculations of the gas flow are based on numerical integration of the full system of stationary Reynolds equations written in Euler variables. To find the coefficients of turbulent diffusion, use is made of the Boussinesq hypothesis on the linear dependence of the components of the tensor of turbulent stresses on the components of the tensor of deformation rates of average motion and two equations of transfer of turbulence characteristics. Details of the calculation technique one can find in the research (Maiorova at all, 2010).

Researches were conducted on 2 versions of devices: with airflows swirling in opposite directions (variant 1) and in one direction (variant 2). Calculated air flow rate G_A through the sprayer unit and swirlers are resulted in table 4.

Swirlers	$G_A, \text{ g/s}$	
	swirling in opposite directions (variant 1)	swirling in one direction (variant 2)
Total	16.3	15.7
Outer	12.0	11.6
Central	4.3	4.1

Table 4. Air mass flow rate - preliminary design

The difference in flow rates values it is possible to explain by the absence of developed reverse zone in variant with opposite swirling and, as consequence, smaller outlet back pressure. Calculations show that, at opposite directions swirling, it is possible to receive higher intensity of turbulence and accordingly the best spray fineness. However thus there is no stable zone of reverse flow. The underpressure area is formed of the device exit behind the central body because of more axial velocity in comparison with variant 2. It will negatively affect stable combustion limits in combustor. More uniform pressure field in a cross-section direction on distance of 20 mm from a nozzle edge, is received in calculation 2.. It should positively affect boundary lines of ignition and lean blowout.

Thus it is possible to conclude, that the scheme with swirling in one direction is more preferable to continue researches and detail burner design.

The calculations carried out revealed the necessity of further air mass flow rate increase. It's necessary for the provision of reliable start and high combustion efficiency.

A number of calculations has been conducted to investigate the interaction of streams from the central and circumferential air swirlers at various swirl parameters. It has been received that the best performance is provided at use of two swirlers with an identical blade angles – on 45° to a device axis In the designed burner the following percentage of air mass flow rates through swirlers has been received: 33 % - in the central, 67 % - in outer (table 5).

Swirlers	$G_A, \text{ g/s}$
Total	37.3
Outer	24.9
Central	12.4

Table 5. Air mass flow rate – final design

At designing of low-pressure injectors a collapse of a fuel bubble is essential danger, especially on low modes. For prevention of this phenomenon, already at a design stage, it is necessary to carry out the calculation of the shape of a fuel film. Fundamental theory of a calculation method was stated in (Chuec S. G., 1993). In research (Vasil'ev at al, 2010) this mathematical model has been applied to calculate the film form generated downstream of dual-orifice pressure-swirl atomizer. It has been shown, that the calculated film shape is in satisfactory agreement with the shape obtained in the experiment. With the specified geometrical parameters of an atomizer, these shapes are determined by the flow rate of liquid through the atomizer.

The simplified system of mass and momentum conservation equations in the coordinate system connected with a film surface taking into account gravity forces was solved by numerical method. Initial data about a film thickness, spray angle, longitudinal and

tangential liquid velocities were set from hydraulic design of an injector. The calculations carried out have shown that on operational modes there is a confident deployment of a fuel bubble. It will allow to provide hit of enough of fuel droplets into plug discharge zone and, as consequence, sufficient area for assured firing of the combustion chamber.

4. Results of the combined burner analysis

4.1 Flow rate characteristics of the burner

Testing of the burner manufactured begins with measurement of flow rate characteristics of injectors in tests without participation of air and their comparison with calculated ones (fig. 3.a). Measurements of the liquid mass flow rate were conducted by firm KROHNE flowmeter (a measurement error <1 %). The air mass flow rate was measured by PROMASS flowmeter. Fluid injection pressure was transduced by AZD pressure sensors. The comparison of experimental and calculated characteristics by air is presented on fig. 3.b. It is possible to consider the concurrence received as comprehensible (taking into account possible errors of manufacturing).

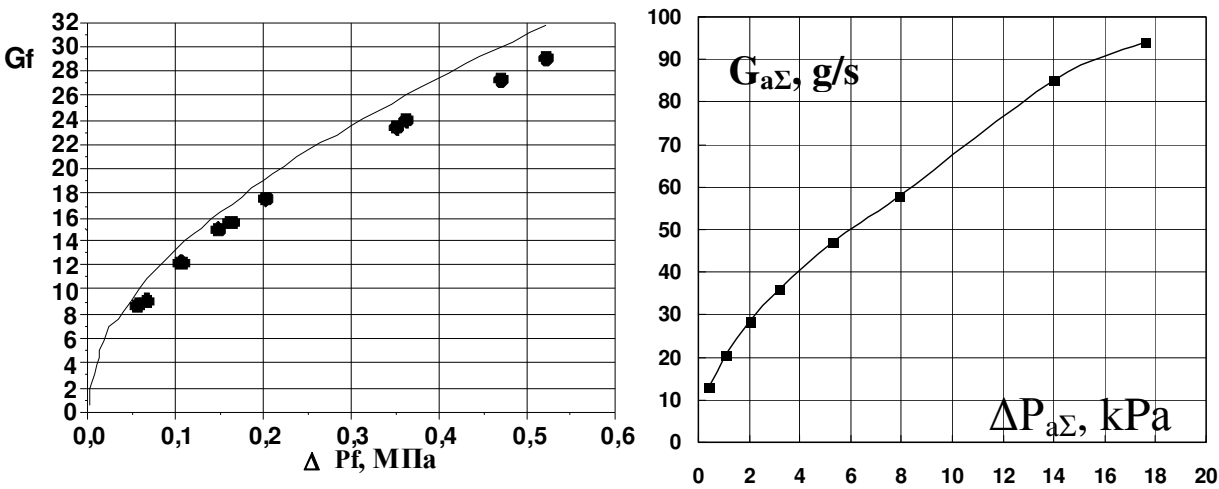


Fig. 3. Mass flow rate characteristics of an injector on kerosene (the outer channel) and air (total); lines - calculation, points - experiment

4.2 The investigation of fuel films without supply of airflows.

As is well known, the form of liquid exposed to an atomization, in an appreciable measure influences the quality of the aerosol received, basically on such parameters as fuel droplets distribution in cross section and a spray angle. In this connection, the complex of cold tests has been continued by investigation of the form of fuel films without supply of airflows. In experiences it was spent laser visualization of a stream. The flow of kerosene film at the outlet from the atomizer nozzle was recorded using a Canon XL-H1 three-matrix color video camera. Photos of the expiration of a fuel film at various mass flow rates and measured spray angles for injectors investigated are resulted on fig. 4 and 5. Operational modes for a pressure-swirl atomizer begin with flow rates corresponding to a photo 4b and above. In this range of flow rates it was possible to reach good stability of a fuel film angle. The photo on fig. 4a visually shows high uniformity of a fuel sheet even on lower modes, usually hard-hitting. For a pressure-swirl atomizer a target range of spray angles - 90-95° and high uniformity of injection are reached without of supply of an airflow.

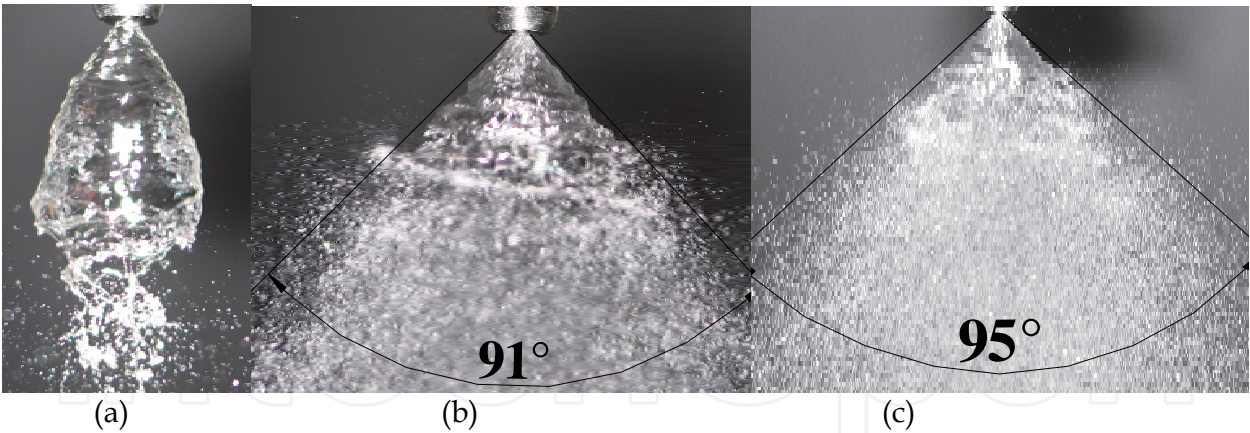


Fig. 4. Photos of the expiration of a kerosene film at various mass flow rates throw the pressure swirl nozzle; a) $G_{f1} = 1.77 \text{ g/s}$, $\Delta P_{f1} = 60 \text{ kPa}$; b) $G_{f1} = 2.7 \text{ g/s}$, $\Delta P_{f1} = 150 \text{ kPa}$; c) $G_{f1} = 3.5 \text{ g/s}$, $\Delta P_{f1} = 286 \text{ kPa}$.

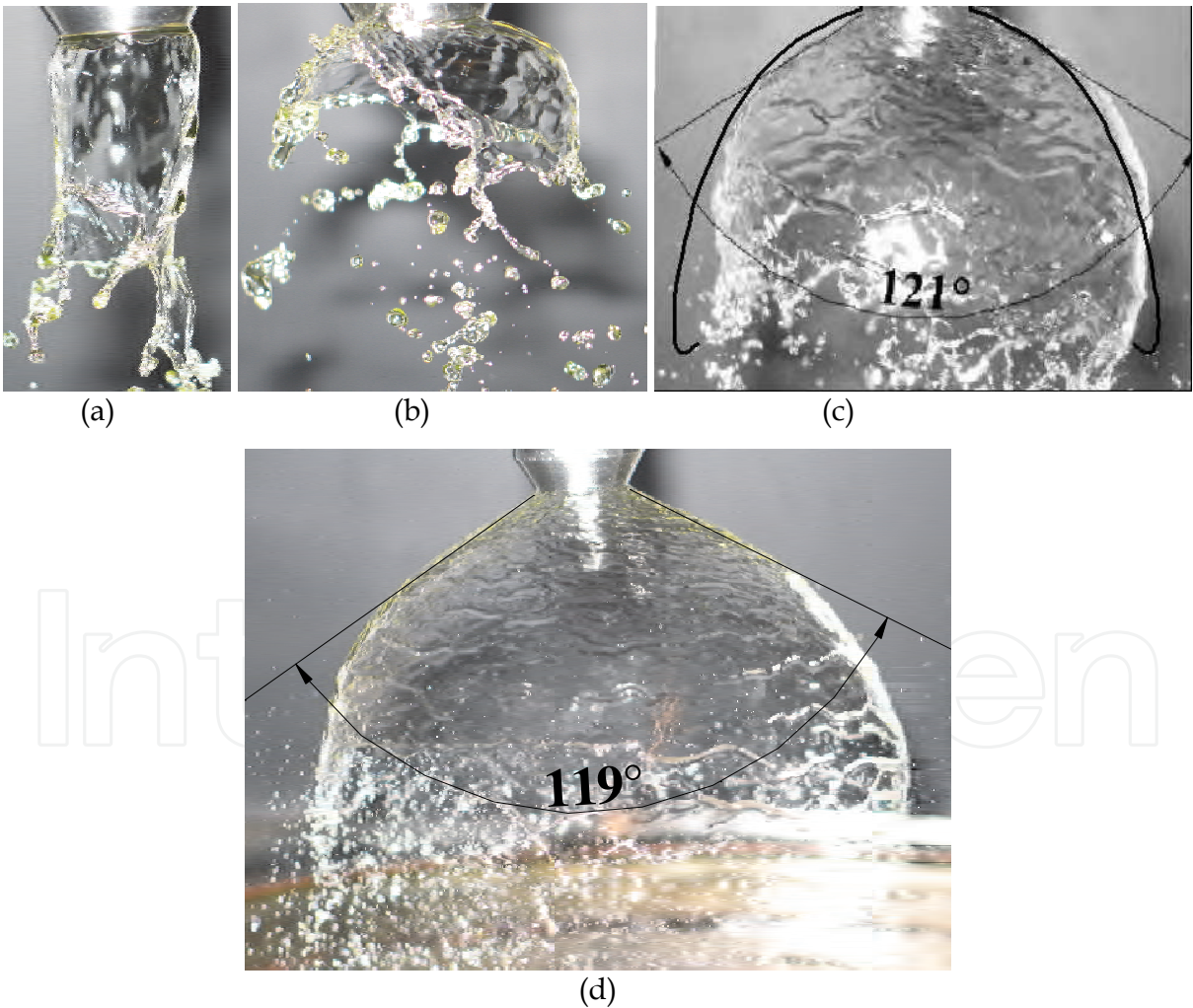


Fig. 5. Photos of the expiration of a kerosene film at various mass flow rates throw the airblast nozzle; a) $G_{f1} = 9.2 \text{ r/c}$, $\Delta P_{f1} = 66 \text{ kPa}$; b) $G_{f2} = 12.3 \text{ r/c}$, $\Delta P_{f1} = 105 \text{ kPa}$; c) $G_{f1} = 17.5 \text{ r/c}$, $\Delta P_{f1} = 202 \text{ kPa}$; line - calculation; d) $G_{f2} = 24.0 \text{ g/s}$, $\Delta P_{f2} = 362 \text{ kPa}$

Photos of the expiration of a fuel film at various flow rates throw the airblast atomizer are presented on fig. 5. The comparison on Fig. 5c shows that the computational technique describes well the experimental data on the configuration of the fuel. Fig. 5c corresponds to underload mode, 5d - mode 100 %, thus spray angle - an order 120° . Substantial growth of fuel film diameter till the moment of its contact to swirled airflows provides reduction of its thickness in a zone of pneumatic spraying. As consequence, the fineness of atomization improves essentially.

Thus for the fuel channel of an airblast injector the spray angle without airflow submission, and the small thickness of a fuel film are received stable on modes. This allows to improve considerably the fineness of atomization even on low engine power settings.

4.3 The comprehensive investigations of the burner with air submission

Comprehensive test of the burner in open space with air submission were carried out. Measurements were conducted on a bench of laser diagnostics. The important parameters characterizing quality of the device performance - value and intensity of paraxial reverse zone were optimized. As a result of tests geometrical parameters of sprayer unit were updated. Axial rules of injectors and swirlers, and also blades angles of swirlers varied. As a result of optimization following blade angles have been chosen: 60° for the central swirler, 45° for the circumferential one. The difference of optimum angles from received in predesign, is connected possibly with distinction of calculation and experimental areas.

When carrying out aerodynamic 3-D calculations of optimized flame sprayer the total air flow through the burner (37.3 g/s), with a following percentage ratio of mass flow rates is received: 33 % - in the central swirler (12.4 g/s), 67 % - in outer one (24.9 g/s).

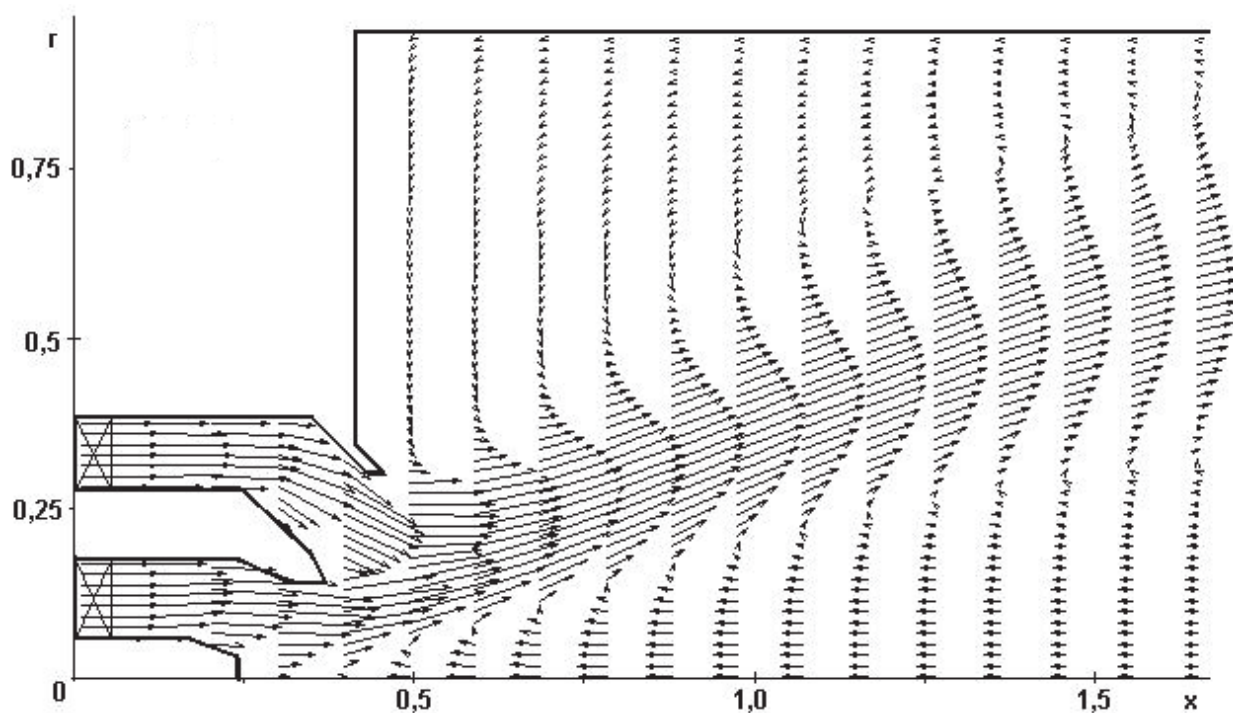


Fig. 6. Calculated vector velocity field behind the burner

Calculated flow pattern in the tube after the burner is given in fig. 6. As one can see from this fig, near the burner axis the advanced zone of reverse flow is formed that should promote the stability of combustion process.

The researches carried out have allowed to conduct comparison on radial distribution of axial and tangential velocities at distance 30 mm behind the burner. Results of imposing of experimental velocity profiles on calculated curves are shown on fig. 7. From the graphs presented on fig. 7, it is possible to draw a conclusion on satisfactory concurrence of calculation and experiment. Let's notice, that the calculated velocity profile is received for air, and experimental for a drop-forming phase formed by the pressure-swirl atomizer. In this connection the experimental velocity curve is a little bit wider then calculated.

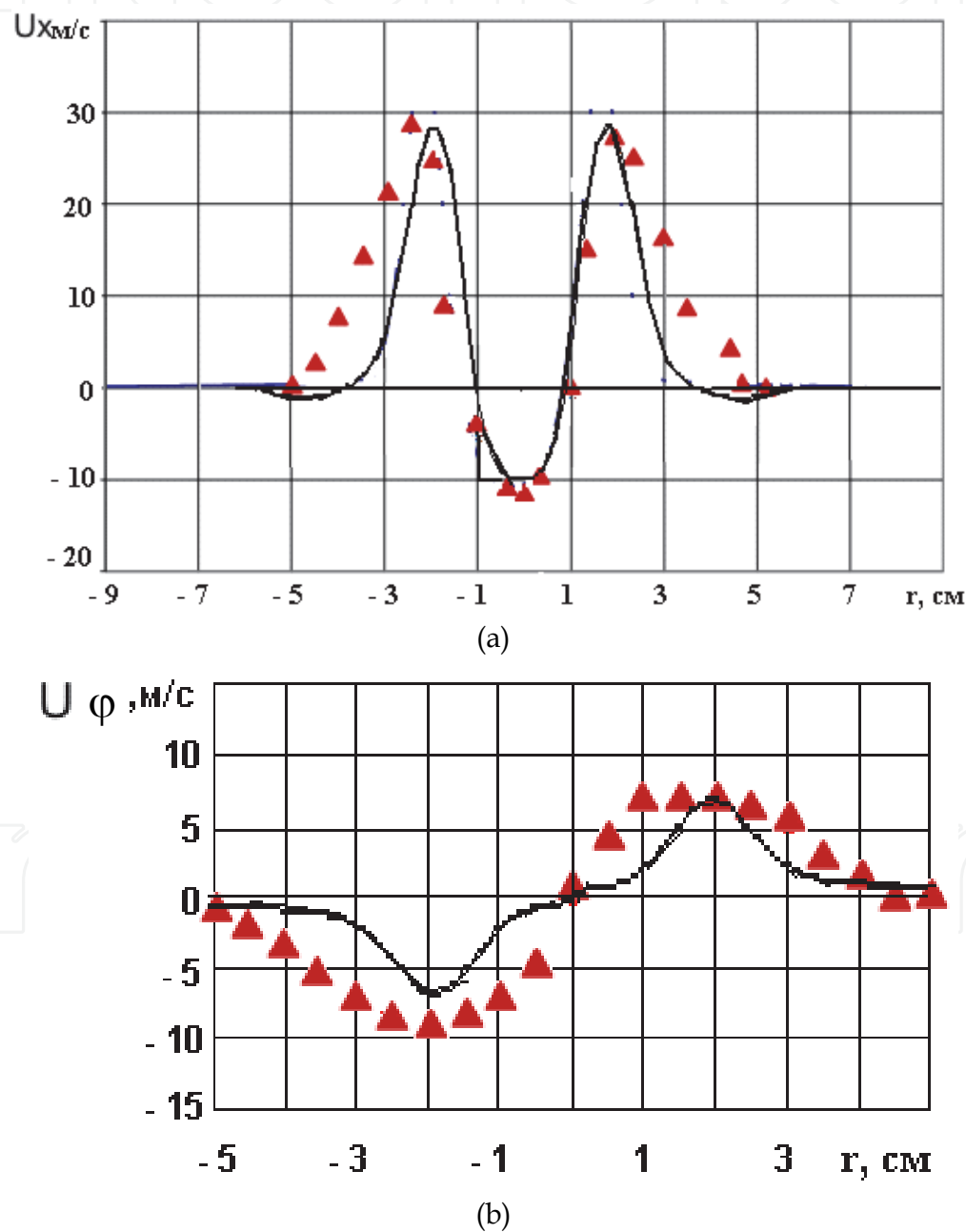


Fig. 7. Distribution of axial (a) and tangential (b) velocities on diameter of a spray; lines – calculation, points – experiment (PDPA measurements)

4.4 Comparative researches of burner performance on different hydrocarbon fuels

Let's estimate now possibility of using of the burner for working on various hydrocarbon fuels - oil and alternative. Calculated performance of a pilot injector at the wake-up mode are given in table 6. The performance of a main injector at the mode 100 % are presented in table 7.

fuel	C _D	ΔP _f , MPa	2θ _R , °	SMD, mkm
Ethanol	0.140	0.893	102.0	19.5
Kerosene TS1	0.146	0.836	100.6	21.7
Ideal diesel	0.186	0.471	90.9	39.7
FAME (biodiesel)	0.195	0.415	86.3	52.8

Table 6. Calculated performance of a pilot injector at the fuel rate 5 g/s

fuel	C _D	ΔP _f , MPa	2θ _R , °	SMD, mkm
Ethanol	0.003	0.335	151.3	41.4
Kerosene TS1	0.003	0.336	152.0	39.8
Ideal diesel	0.003	0.353	148.6	58.6
FAME (biodiesel)	0.003	0.356	144.3	81.4

Table 7. Calculated performance of a main injector at the fuel rate 25 g/s without air supply

As one can see from table 7, flow rate characteristics of the big main injector practically do not depend on fuel viscosity. Discharge coefficients are identical for all fuels and the difference of injection pressure is determined only by a difference of density. Values of spray root angles are very close for all fuels, and real sizes of droplets will be mainly air streams dependent. The pilot injector performance (table 6) to a greater extend depend on a fuel kind. The deviation of discharge coefficients from one for a diesel is within 24 %, the dispersion of spray angles - within 12 %. As a whole, however, the injector provides comprehensible performance on regimes on wake-up and underload modes for all kind of fuel observed. Let's consider also results of calculation of the fuel film shape for various fuels. The film thickness on an exit from the main injector is essentially more than on an exit from the pilot injector. The fuel kind can exert the greatest influence on the deployment of a fuel bubble in the case of the main injector.

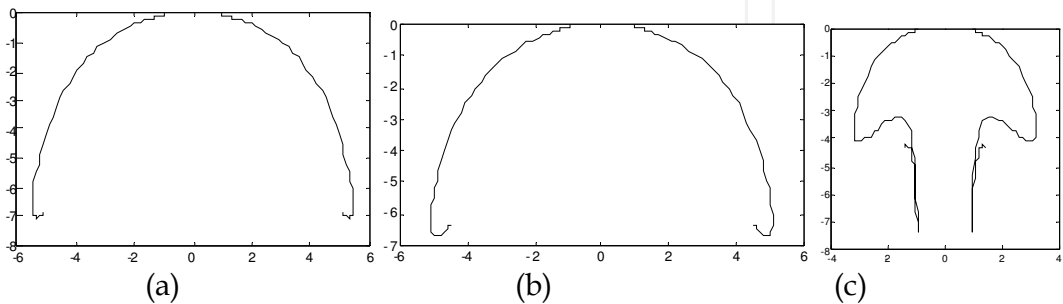


Fig. 8. Calculated shape of fuel film without supply of air; G_f=17.5 g/s; a – ethanol, b – kerosene, c - biodiesel

Calculated shapes of fuel film downstream of main atomizer without supply of air and with supply of air are given in fig. 8 and 9 respectively. Fuel mass flow rate corresponds to underload mode. The nozzle radius is assumed as characteristic dimension.

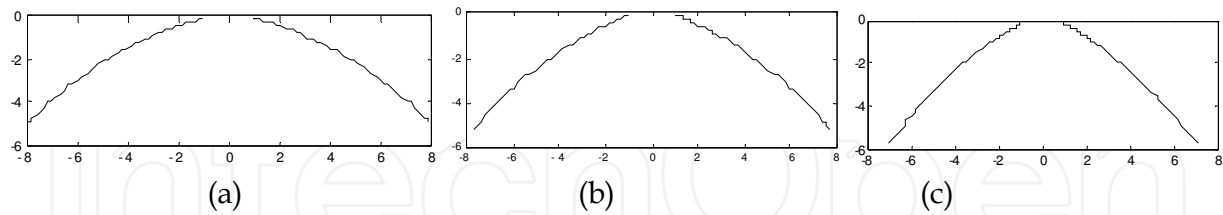


Fig. 9. Calculated shape of fuel film with supply of air; $G_f=17.5\text{ g/s}$; a – ethanol, b – kerosene, c - biodiesel

As one can see from fig. 8, in the absence of air supply for the regime considered the shape of fuel spray depend on fuel kind. In case of most viscous of them – a biodiesel - the fuel spray does not deploy. However, during air injection the shape of fuel film is determined, basically, by the airflow. Apparently from fig. 9, confident disclosing of a fuel spray for fuels as with normal, and the raised viscosity is observed in this case.

In fig. 10 - 12 the results of comparative test of the burner at normal conditions on different hydrocarbon fuels (PDPA measurements) are presented during air injection for wake-up mode (centrifugal nozzle works only) and underload mode (both nozzles work). At the underload mode measurements for mix of diesel fuel with rapeseed oil in ratio 50% - 50% were carried out too. Physical properties of this mix are: $\rho_f = 867\text{ kg/m}^3$, $\nu_f = 12\text{ mm}^2/\text{s}$. Apparently from Fig. 10-11, the difference of the droplets sizes or diesel fuel and kerosene is appreciable weakly. Diesel-oil droplets are large-scale near the axis. However their sizes are in the range of target values. Values of SMD average along the cross section are 40-60 mkm. Values of volumetric concentration are neighbour for all fuels. The flow structure as it is visible from fig. 12, is self-similar. This result shows, that at flow rates ratio used the atomization is determined mainly by an airflow.

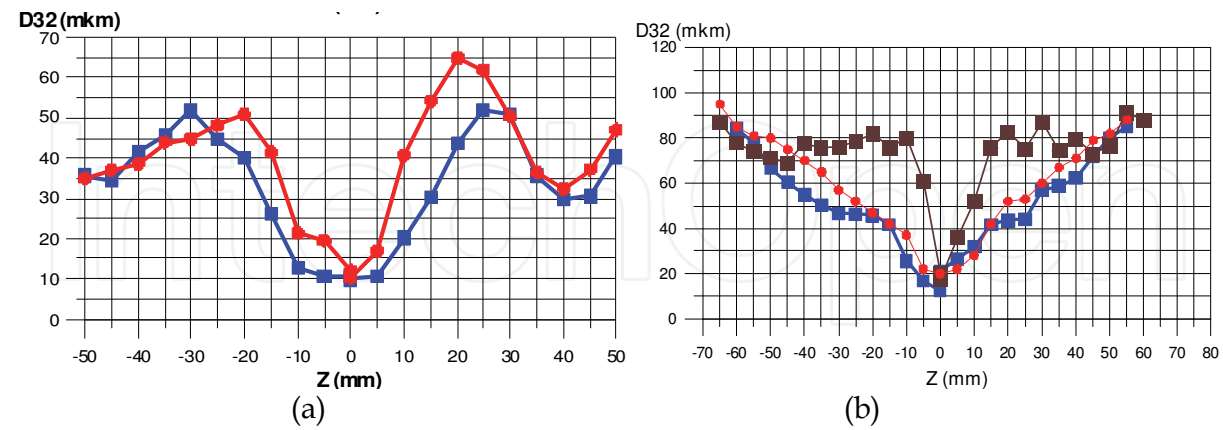


Fig. 10. Distribution of the droplets sizes on diameter of a spray; a) wake-up mode, $\Delta P_a=3\text{ kPa}$, $G_f=5\text{ g/s}$; b) underload mode, $\Delta P_a=3\text{ kPa}$, $G_f=20\text{ g/s}$; -●- diesel; -■- kerosene; -◆- diesel - oil mix

The photo of fuel-air spray for underload mode is given in fig. 13. The spray angle for diesel and kerosene practically does not depend on a fuel kind that proves to be true also concentration structures (fig. 11), and makes an order 90° . It corresponds to target value of

this parameter. Apparently from Fig. 13b the spray angle makes more than 80° even for such viscous fuel, because the spraying is determined by air streams.

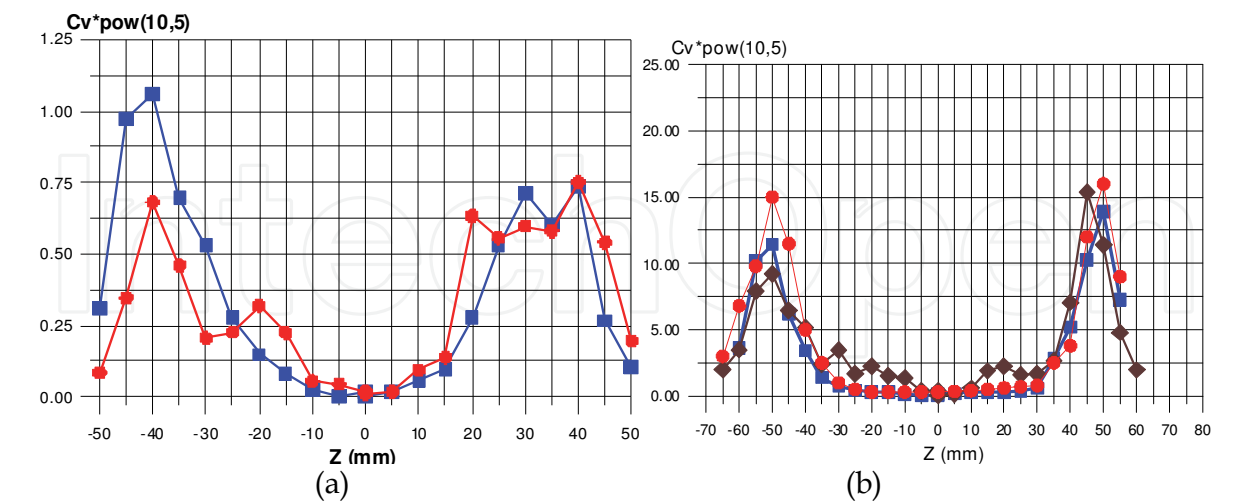


Fig. 11. Distribution of the volumetric concentration of a liquid fuel on diameter of a spray; a) wake-up mode, $\Delta P_a=3$ kPa, $G_f=5$ g/s; b) underload mode, $\Delta P_a=3$ kPa, $G_f=20$ g/s; -●-diesel; -■-kerosene; -◆- diesel -oil mix

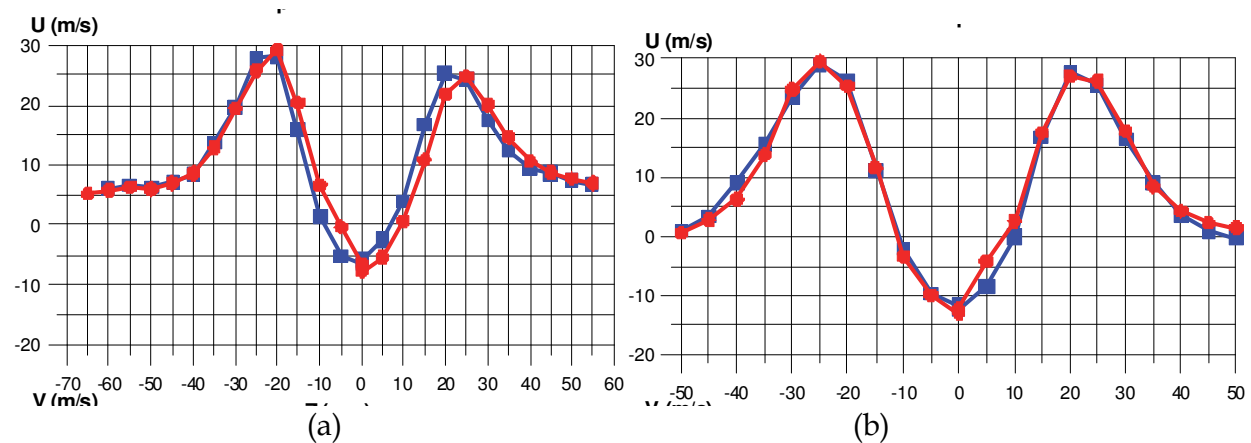


Fig. 12. Distribution of the axial velocity on diameter of a spray; a) wake-up mode, $\Delta P_a=3$ kPa, $G_f=5$ g/s; b) underload mode, $\Delta P_a=3$ kPa, $G_f=20$ g/s; -●-diesel; -■- kerosene

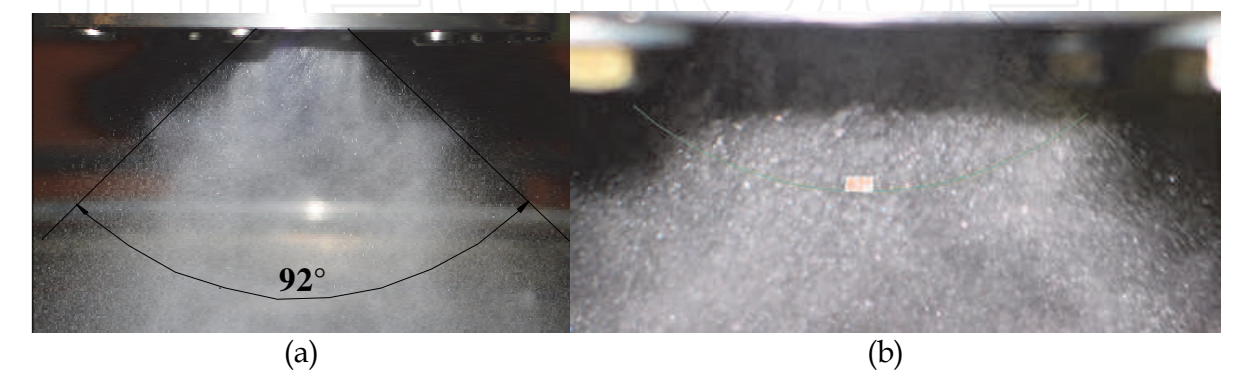


Fig. 13. The photo of fuel-air spray; $\Delta P_a=3$ kPa, $G_f=20$ g/s; a - diesel, kerosene; b - diesel -oil mix

Results of the present section show that the designed dual-orifice atomizer can be used for different fuels, both for oil, and for alternative. In addition injection valve modernization can be necessary only.

4.5 Tests of a burner with the low-emission combustion chamber compartment

For fire tests of a burner with the combustion chamber compartment the flame tube with permeability 4281 mm² was used. The kerosene TS1 was used as fuel. Boundary lines of the flame blowout (fig. 14) were determined only on one pilot channel. It is possible to assume, that connection of the second channel of a burner will allow to expand a zone of a stable running of the chamber even more. The received blowout boundary line shows, that the chamber steadily works in a range coefficient of air excess α_c from 1 to 6.5 and air volume flow rate Q_c up to 0.45 m³/s at underpressure in chamber $P_c = 0.08$ MPa. This operation mode corresponds to altitude of an order of 2 km.

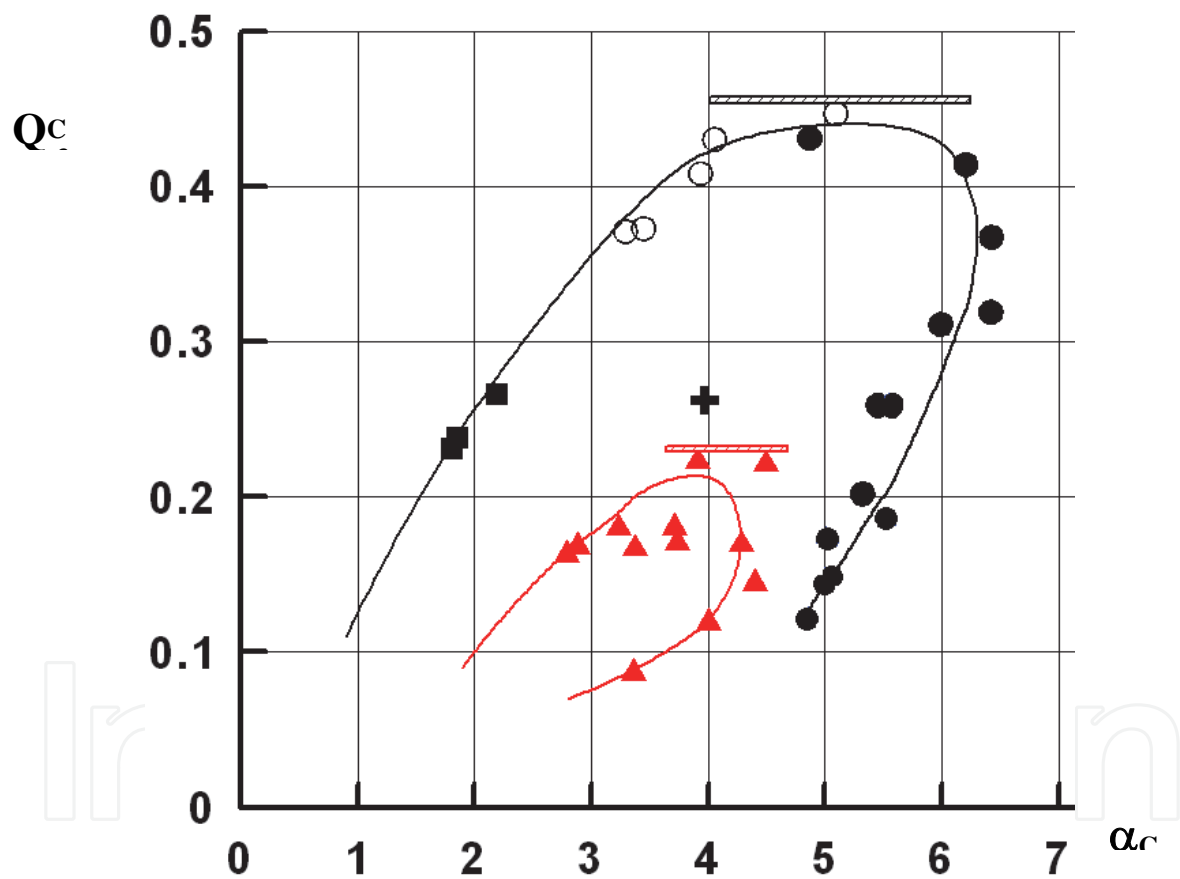


Fig. 14. Boundary lines of ignition and blowout in the combustion chamber compartment, the plug 2 J, $H \approx 2$ km, $T_C^* = 280$ K, • - lean blowout, O - rich blowout, ▲ - wake-up, ■ - there is no rich blowout, + - the point of temperature field taking-out

The area boundary reaches satisfactory values on α_c , and comprehensible values on Q_c . The ignition domain boundary is sufficient on the square for assured firing of the combustion chamber. The given result allows to assert, that blowout characteristics in earth conditions will appear at least not worse received. Flame photos at various α_c are shown in fig. 15.

Also the temperature fields behind an exit from transition liner in a pipe of diameter 110 mm have been taken out under various α_C . The temperature field received has a symmetric appearance and small non-uniformity on value of temperature - the minimum value differs from maximum on 70 K. The temperature distribution on one radius is resulted in fig. 16.

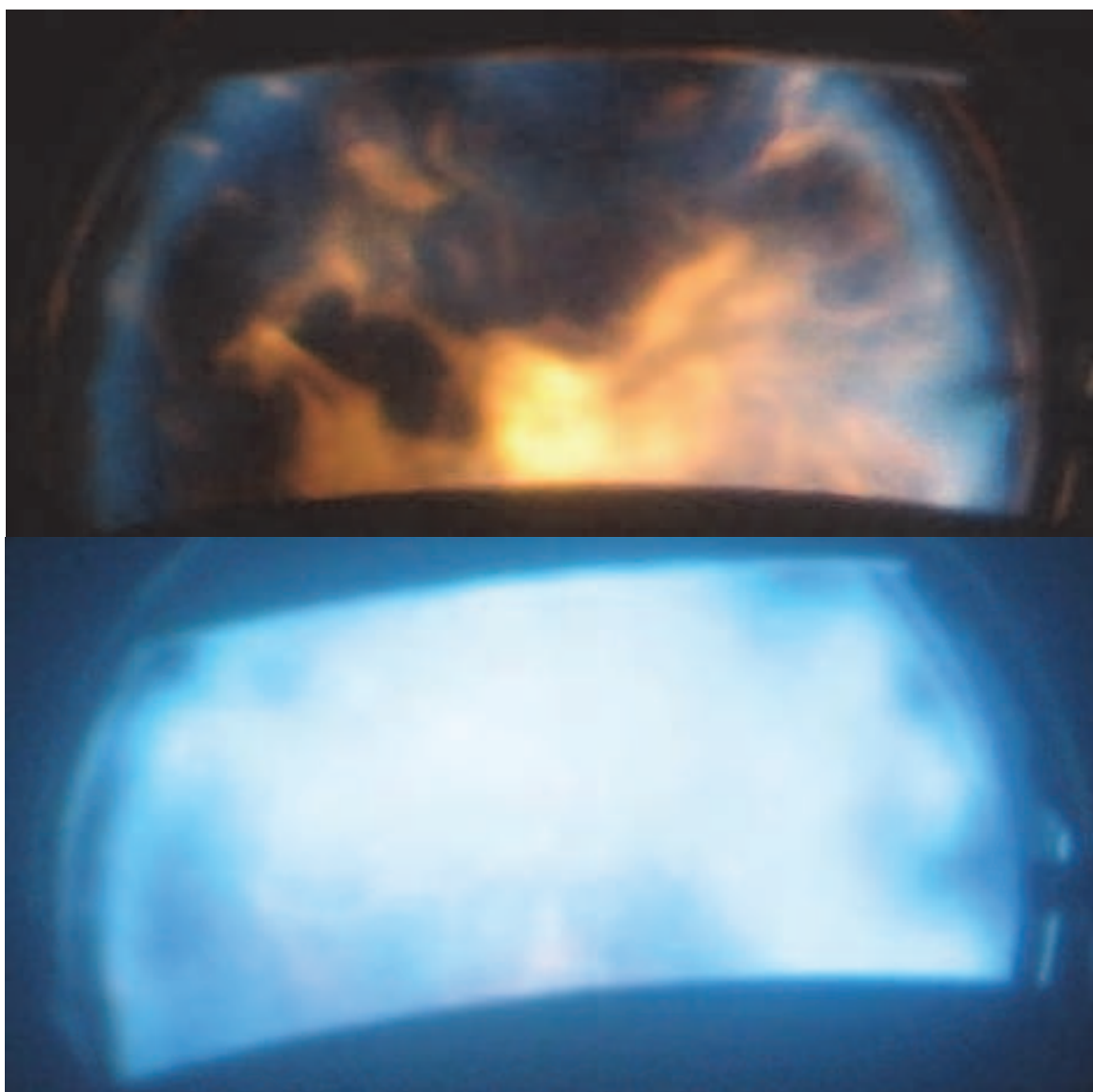


Fig. 15. Flame photos at various α_C .

Integration of this curve allows to receive mass average value of temperature $T_{av} = 575K$.

The dependence of combustion efficiency and average temperature behind the transition liner on air excess coefficient is presented in fig. 17. The combustion efficiency was calculated on value of temperature according to the work (Kulagin, 2003).

On the basis of the spent experiments it is possible to assert, that the burner developed has shown comprehensible characteristics. In particular wide side-altars of the stable combustion, assured firing of the combustion chamber, uniform enough field of gas temperature on an exit and satisfactory combustion efficiency, taking into account that tests occurred on a regime close to earth wake-up mode.

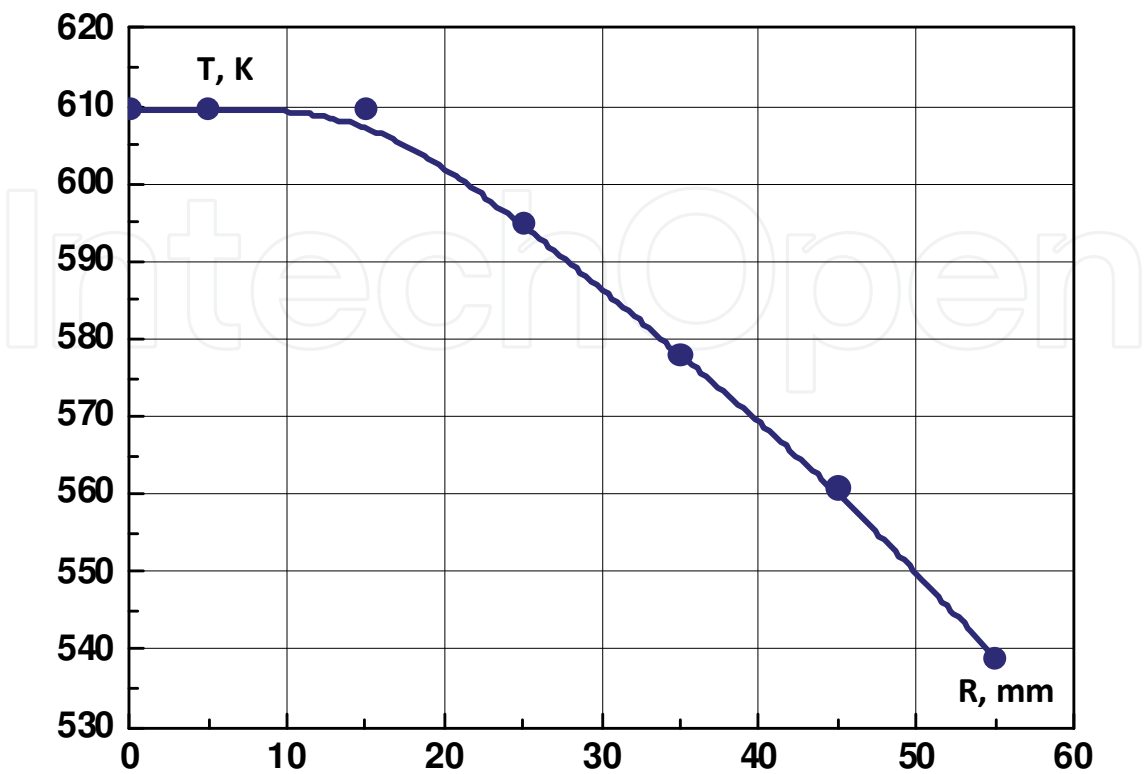


Fig. 16. Radial temperature distribution; $\alpha_C = 4$; $Q_C = 0.28$.

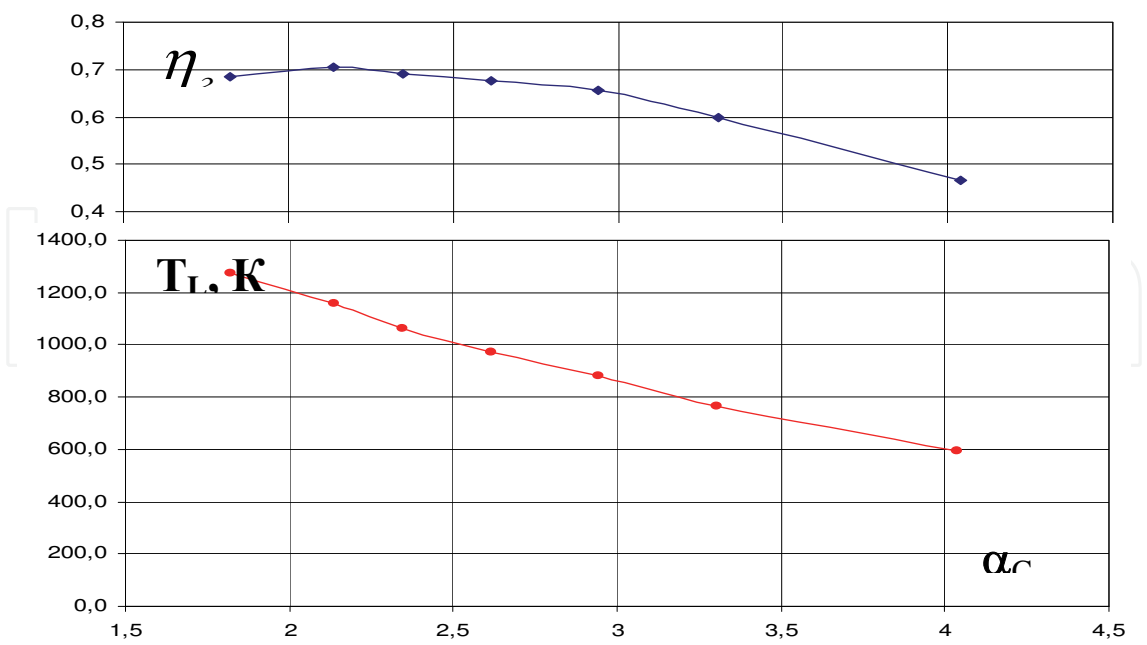


Fig. 17. The dependence of combustion efficiency and average temperature behind the transition liner on air excess.

5. Summary

The designing, manufacturing and test of individual injectors and the burner as a whole for low-emission combustion chambers of gas-turbine engine or gas-turbine plant is executed. The present work represents a complex of target researches on design-experiment basing of shape of the sprayer unit for low-emission combustors on fuels as usual, as of the increased viscosity (kerosene, ethanol, diesel, biodiesel).

The dual-orifice (on fuel) burner of the combined centrifugal-airblast scheme is proposed. Nozzles of atomizers place concentrically. The low-rate pilot channel (pressure swirl nozzle) is installed on a burner axis. The main channel – airblast nozzle is located between two air swirlers.

Hydraulic design of pilot channel and numerical 3D modeling of air channels of the burner are carried out. Geometrical parameters of the burner and blades angles of swirlers were chosen. These parameters were optimized during comprehensive test of the burner in open space with air submission.

On the basis of calculation researches two heads of injectors are designed and made: centrifugal and airblast for the combined burner.

The investigation of fuel films without supply of airflows is carried out. For a pressure-swirl atomizer a target range of spray angles - 90-95° and high uniformity of injection are reached. For the fuel channel of an airblast injector the spray angle without airflow submission, and the small thickness of a fuel film are received stable on modes. This allows to improve considerably the fineness of atomization even on low engine power settings.

The comparative researches of burner performance on different hydrocarbon fuels are carried out. It's shown that at fuel-air flow rates ratio used the atomization is determined mainly by an airflow. Schemes of devices worked out provide the adjacency of aerosol characteristics for combustibles investigated. Values of Sauter Mean Diameter average 40-60 mkm. The spray angle when both injectors working with air supply makes an order 90°. Results of the research show that the designed dual-orifice atomizer can be used for different fuels, both for oil, and for alternative.

Fire tests of a burner with the low- emission combustion chamber are conducted. It is possible to assert, that the burner developed has shown comprehensible characteristics. In particular wide side-altars of the stable combustion, assured firing of the combustion chamber, uniform enough field of gas temperature on an exit and satisfactory combustion efficiency.

Results of present work are protected by the Patent of the Russian Federation (Vasil'ev et al. 2009).

6. Notation

C_d - discharge coefficient of injector

C_v - volumetric concentration of a liquid fuel, kg/m³

D_{32} - droplet mean Zauter diameter, average along the circumference, m

G - mass flow rate, kg/s

P - pressure, Pa

Q - air volume flow rate, m³/s

ΔP - injection pressure, Pa

SMD - droplet mean Zauter diameter average along the whole cross section, m

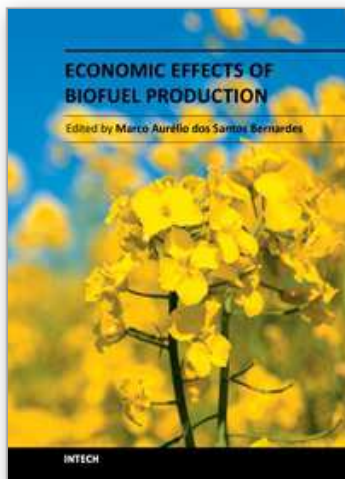
T – temperature, K
 U – velocity, m/s
 α - coefficient of air excess
 η - combustion efficiency
 μ - dynamic viscosity, kg/(m·s)
 ν - kinematic viscosity, m²/s
 θ_R - spray root angle, °
 ρ - density, kg/m³
 σ - surface tension coefficient, N/m

Subscripts

a – air
 C – combustion chamber
 f - liquid fuel

7. References

- Chuec S. G. (1993) Numerical Simulation of Nonswirling and Swirling Annular Liquid Jets. *AIAA Journal*. Vol.31. No.6. P.1022-1027.
- Dityakin Yu. F., Klyachko L. A., Novikov B. V. and V. I. Yagodkin. (1977). *Spraying of Liquids* (in Russian), Mashinostroenie, Moscow.
- Kulagin V.V. (2003). *The theory calculation and designing of aircraft engines and power plants*. (in Russian), Mashinostroenie, Moscow.
- Lefebvre A.H. (1985). *Gas Turbine Combustion*, Hemisphere Publishing corporation, Washington, New York, London.
- Lefebvre A.H. (1989). *Atomization and Sprays*, Hemisphere Publishing corporation, New York.
- Anna Maiorova, Aleksandr Sviridenkov and Valentin Tretyakov (2010). The investigation of the mixture formation upon fuel injection into high-temperature gas flows. *Fuel Injection*. Edited by D. Siano. Published by Sciyo. P.121 - 142. ISBN 978-307-116-9.
- Patankar S. (1980). *Numerical Heat Transfer and Fluid Flow*, Hemisphere Publishing, New York.
- Vasil'ev A. Yu. (2007). Comparison of performance s of various types of the injectors working with use of an air stream. (in Russian). The bulletin of Samara State Aerospace University. No 2(13). P. 54-61.
- A.Yu. Vasil'ev, A. I. Maiorova, A. A. Sviridenkov and V. I. Yagodkin (2009). Patent of Russian Federation No 86279.
- A.Yu. Vasil'ev, A. I. Maiorova, A. A. Sviridenkov and V. I. Yagodkin (2010). Formation of Liquid Film Downstream of an Atomizer and Its Disintegration in Gaseous Medium. *Thermal Engineering*. Vol. 57, No. 2. P. 151-154. ISSN PRINT: 0040-6015. ISSN ONLINE: 1555-6301.



Economic Effects of Biofuel Production

Edited by Dr. Marco Aurelio Dos Santos Bernardes

ISBN 978-953-307-178-7

Hard cover, 452 pages

Publisher InTech

Published online 29, August, 2011

Published in print edition August, 2011

This book aspires to be a comprehensive summary of current biofuels issues and thereby contribute to the understanding of this important topic. Readers will find themes including biofuels development efforts, their implications for the food industry, current and future biofuels crops, the successful Brazilian ethanol program, insights of the first, second, third and fourth biofuel generations, advanced biofuel production techniques, related waste treatment, emissions and environmental impacts, water consumption, produced allergens and toxins. Additionally, the biofuel policy discussion is expected to be continuing in the foreseeable future and the reading of the biofuels features dealt with in this book, are recommended for anyone interested in understanding this diverse and developing theme.

How to reference

In order to correctly reference this scholarly work, feel free to copy and paste the following:

Anna Maiorova, Aleksandr Sviridenkov, Valentin Tretyakov, Aleksandr Vasil'ev and Victor Yagodkin (2011). The Development of the Multi - Fuel Burner, Economic Effects of Biofuel Production, Dr. Marco Aurelio Dos Santos Bernardes (Ed.), ISBN: 978-953-307-178-7, InTech, Available from:
<http://www.intechopen.com/books/economic-effects-of-biofuel-production/the-development-of-the-multi-fuel-burner>

INTECH
open science | open minds

InTech Europe

University Campus STeP Ri
Slavka Krautzeka 83/A
51000 Rijeka, Croatia
Phone: +385 (51) 770 447
Fax: +385 (51) 686 166
www.intechopen.com

InTech China

Unit 405, Office Block, Hotel Equatorial Shanghai
No.65, Yan An Road (West), Shanghai, 200040, China
中国上海市延安西路65号上海国际贵都大饭店办公楼405单元
Phone: +86-21-62489820
Fax: +86-21-62489821

© 2011 The Author(s). Licensee IntechOpen. This chapter is distributed under the terms of the [Creative Commons Attribution-NonCommercial-ShareAlike-3.0 License](https://creativecommons.org/licenses/by-nc-sa/3.0/), which permits use, distribution and reproduction for non-commercial purposes, provided the original is properly cited and derivative works building on this content are distributed under the same license.

IntechOpen

IntechOpen